Available online at www.sciencedirect.com

SCIENCE DIRECT

Developmental Biology 289 (2006) 30 – 43

DEVELOPMENTAL BIOLOGY

www.elsevier.com/locate/ydbio

Novel heterochronic functions of the *Caenorhabditis elegans* period-related protein LIN-42

Jason M. Tennessen, Heather F. Gardner, Mandy L. Volk, Ann E. Rougvie *

Department of Genetics, Cell Biology and Development, University of Minnesota, 6-160 Jackson Hall, 321 Church St. SE, Minneapolis, MN 55455, USA

Received for publication 11 August 2005, accepted 27 September 2005
Available online 21 November 2005

Abstract

LIN-42, the *Caenorhabditis elegans* homolog of the Period (Per) family of circadian rhythm proteins, functions as a member of the heterochronic pathway, regulating temporal cell identities. We demonstrate that *lin-42* acts broadly, timing developmental events in the gonad, vulva, and sex myoblasts, in addition to its well-established role in timing terminal differentiation of the hypodermis. In the vulva, sex myoblasts, and hypodermis, *lin-42* activity prevents stage-specific cell division patterns from occurring too early. This general function of timing stage-appropriate cell division patterns is shared by the majority of heterochronic genes; their mutation temporally alters stage-specific division patterns. In contrast, *lin-42* function in timing gonad morphogenesis is unique among the known heterochronic genes: inactivation of *lin-42* causes the elongating gonad arms to reflex too early, a phenotype which implicates *lin-42* in temporal regulation of cell migration. Three additional isoforms of *lin-42* are identified that expand our view of the *lin-42* locus and significantly extend the homology between LIN-42 and other PER family members. We show that, similar to PER proteins, LIN-42 has a dynamic expression pattern; its levels oscillate relative to the molts during postembryonic development. Transformation rescue studies indicate *lin-42* is bipartite with respect to function. Intriguingly, the hallmark PAS domain is dispensable for LIN-42 function in transgenic animals.

Keywords: *lin-42*; Period; Heterochronic; Gonad morphogenesis; Circadian rhythm; Developmental timing

Introduction

Metazoan development requires temporal coordination of cell division and tissue differentiation. In *Caenorhabditis elegans*, the heterochronic gene pathway mediates temporal control of postembryonic development as the worm progresses through four larval stages (L1–L4) to the adult (for review, see Rougvie, 2005). Disruption of a heterochronic gene causes the temporal identity of developing tissues to be altered. For example, lateral hypodermal seam cells undergo a characteristic series of stage-specific cell divisions before terminally differentiating during the final molt (Fig. 1A). In precocious mutants, such as *lin-14(loss-of-function (lf))* and *lin-28(lf)*, seam cells inappropriately adopt temporal identities normally assigned to later larval stages, resulting in terminal differentiation during the L3 molt, one stage too early (Ambros and Horvitz, 1984). In contrast, seam cells of *lin-4(lf)* and *lin-29(lf)* mutants stall in their progression through temporal fates, resulting in a reiteration of earlier cell identities during later stages such that terminal differentiation fails to occur at the L4 molt (Ambros and Horvitz, 1984; Chalfie et al., 1981).

In general, heterochronic genes act as a series of switches that are thrown stage specifically to allow cell identities to proceed to the subsequent temporal fate. In these cases, loss-of-function and gain-of-function mutations in a given gene cause the opposite temporal transformation (precocious versus retarded development). The heterochronic gene(s) responsible for gating exit from, or entry into, a particular temporal fate undergo dramatic changes in expression during a specific stage, thereby triggering temporal progression. For example, expression of the *lin-4* microRNA (miRNA) is upregulated during the mid-L1 stage of wild type and inhibits productive translation of LIN-14 and LIN-28 mRNAs by binding sites of partial complementarity in their 3′UTRs (Feinbaum and Ambros, 1999; Lee et al., 1993; Moss et al., 1997; Olsen and Ambros, 1999; Wightman et al., 1993). The

* Corresponding author. Fax: +1 612 626 6140.
E-mail address: rougvie@cbs.umn.edu (A.E. Rougvie).

0012-1606/$ - see front matter © 2005 Elsevier Inc. All rights reserved.
doi:10.1016/j.ydbio.2005.09.044

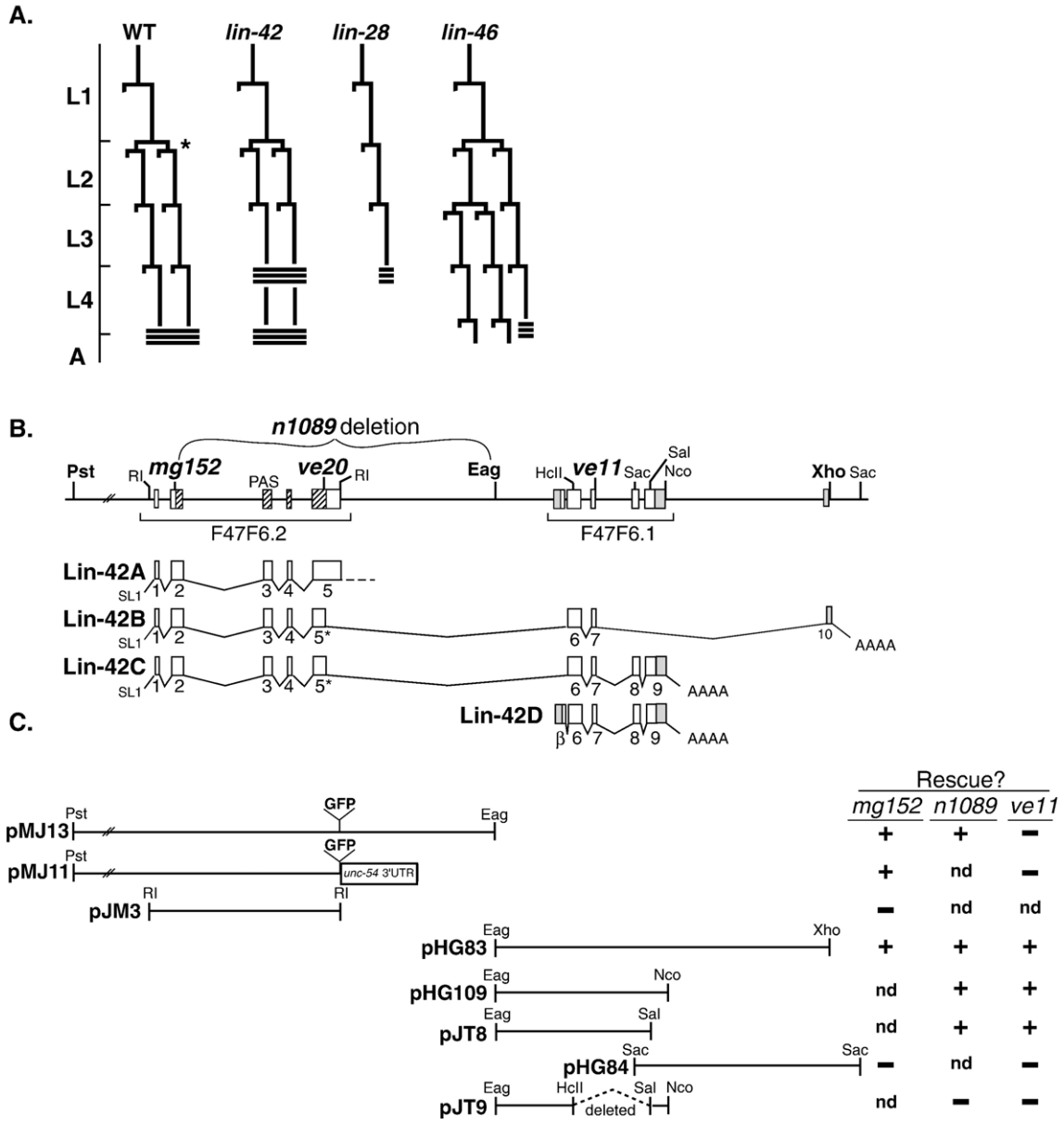

Fig. 1. Diagrams of seam lineage, *lin-42* locus, and transformation rescue constructs. (A) Representative seam cell lineages are shown for wild-type and selected mutants (Abrahante et al., 1998; Ambros and Horvitz, 1984; Pepper et al., 2004). A proliferative division at the start of the L2 stage (asterisk) increases seam cell number from 10 to 16 in wild type. Triple horizontal bars indicate synthesis of adult-type cuticle containing alae. *lin-46* mutants execute a combination of L2 and L3 type divisions at the L2 molt and seam cells sometimes fail to terminally differentiate at the L4 molt. (B) Genomic structure of *lin-42*. Boxes indicate exons. Exon 5* is an alternatively spliced form of exon 5. The region encoding the PAS domain is hatched. Double diagonal lines indicate an area not drawn to scale. The positions of four *lin-42* mutant lesions are shown along with restriction enzyme sites used in clone construction. The "upstream region" extends from Pst to Eag and the "downstream region" from Eag to Xho. Identified *lin-42* transcripts are shown below with untranslated regions in grey. Multiple 3′ ends were found for Lin-42D. (C) Summary of the ability of constructs to rescue the precocious alae defect of *lin-42* alleles (see Table 1). "+" Indicates rescue and "−" indicates failure to rescue. pJM3 results are from Jeon et al. (1999).

resulting decay in LIN-14 and LIN-28 levels during early larval stages causes seam cells to transit from L1 to L2 to L3 specific identities (Ambros and Horvitz, 1987; Moss et al., 1997; Ruvkun and Giusto, 1989; Seggerson et al., 2002). When *lin-4* is absent, these proteins remain present, and seam cells reiterate the L1 stage cell division pattern in subsequent larval stages (Arasu et al., 1991; Chalfie et al., 1981). Conversely, when expressed too early, *lin-4* causes premature expression of the adult fate (Feinbaum and Ambros, 1999).

A similar mechanism specifies temporal transitions later in development. Increased expression of the *let-7* miRNA during the L3/L4 leads to downregulation of targets including LIN-41, allowing accumulation of the LIN-29 transcription factor, which triggers seam cell differentiation at the L4 molt (Bettinger et al., 1996; Reinhart et al., 2000; Rougvie and Ambros, 1995; Slack et al., 2000).

The hypodermal expression patterns of most heterochronic gene proteins follow a paradigm similar to LIN-14, LIN-28, LIN-41, and LIN-29; they accumulate during a subset of larval

stages, and their appearance (e.g., LIN-29) or disappearance (e.g., LIN-14, LIN-28, LIN-41) correlates with changes in temporal identity. LIN-42 appears to be an exception to this general rule; it is expressed during each larval stage (Jeon et al., 1999; this work). *lin-42* loss-of-function mutations cause precocious seam cell differentiation at the L3 molt (Fig. 1A; Abrahante et al., 1998; Liu, 1990). Molecular cloning revealed *lin-42* encodes the worm homolog of the Period (Per) family of proteins (Jeon et al., 1999), which play key roles in circadian rhythm regulation in flies and mammals (reviewed in Glossop and Hardin, 2002). Intriguingly, similarity of *lin-42* to per extends beyond protein homology; both *per* and *lin-42* mRNA levels oscillate relative to recurring events. Oscillations in Per message levels are synchronized to the daily light–dark cycle (Hardin et al., 1990), while *lin-42* mRNA levels are coordinated with the four molts, peaking during each intermolt (Jeon et al., 1999). This cyclical expression pattern suggests that *lin-42* may play multiple or reiterative roles during larval development.

The L1, L2, and L3 stage seam cell divisions appear wild type in *lin-42* mutants (Fig. 1A), suggesting that *lin-42* function is restricted to later development in this lineage. However, L2 stage-specific defects were revealed when *lin-42(n1089)* was placed in combination with *lin-14(n179*ts*)* (Liu, 1990). When *lin-14(n179*ts*)* animals are raised at the permissive temperature (15°C), their seam cells execute a wild-type division pattern. In contrast, seam cells in *lin-14 (n179*ts*)*; *lin-42(n1089)* double mutants skip a proliferative division at the start of the L2 stage. This phenotype is similar to *lin-28* null mutants (Ambros and Horvitz, 1984) and suggests that *lin-42* plays an early role to time this division (Fig. 1A).

In contrast to *lin-28(lf)* single mutants and *lin-42*; *lin-14* double mutants, *lin-46* and *daf-12* single mutants reiterate the L2 stage proliferative division at later stages (Fig. 1A). LIN-46 is a putative scaffold protein for multiprotein complexes, and its loss of function bypasses the need for LIN-28 activity (Pepper et al., 2004). DAF-12 is a nuclear hormone receptor that mediates the choice between reproductive development and entry into dauer diapause at the end of the second larval stage (Antebi et al., 1998, 2000). The relationship between *lin-42* and these two genes relative to control of the proliferative L2 division needs to be examined.

Previous analyses of *lin-42* mutants revealed developmental timing defects only in the hypodermis, suggesting that LIN-42 is a cell type-specific regulator of temporal identity. However, we present evidence that none of the six previously described *lin-42* alleles is a genetic null and demonstrate that LIN-42 has a broader role in control of developmental time, specifying temporal cell identities in multiple tissues, including the gonad. Three additional isoforms of *lin-42* are described, revealing homology of *lin-42* with Per family members that extends beyond the hallmark PAS domain, a predicted protein interaction domain. Remarkably, genomic constructs encoding the C-terminal homology region, but not the PAS domain, are sufficient to provide *lin-42* function.

Materials and methods

Nematode strains and genetics

Nematode growth and maintenance, at 20°C unless noted otherwise, were as described in Sulston and Hodgkin (1988). Alleles used but not specified elsewhere in text: *lin-29(n546)* (Ambros and Horvitz, 1984), *lin-4(e912)* (Chalfie et al., 1981), *lin-46(ma174)* (Pepper et al., 2004), *let-7(mn112)* (Meneely and Herman, 1981), *sqt-1(sc13)* (Cox et al., 1980), *unc-3(e151)*, *unc-4(e120)*, *unc-76(e911)* (Brenner, 1974).

For the complementation analysis between *ve11* and *mg152*, *ve11 unc-4/++* males were mated with *mg152* hermaphrodites. All 22 *ve11 unc-4/mg152+* cross progeny exhibited the *lin-42* Dpy and Egl phenotypes, while all phenotypically wild-type cross progeny were *mg152* heterozygotes.

Molecular biology

PCR-based sequencing of *n1089* DNA identified a 4883-bp deletion beginning in exon 2, 419 bp after the start codon. The *ve11* lesion was found by PCR-based sequencing all exons and intron/exon boundaries.

Lin-42B and C were identified using 3′RACE as described (Gissendanner et al., 2004). Lin-42D RACE experiments were performed with the Ambion First Choice RLM-RACE kit. *lin-42*-specific primers used in the primary and secondary rounds of 3′RACE were AR81 5′-CTTCACTTTCATCACCAAGC-3′ and AR82 5′-GATTCCATACCTTGGTCTCC-3′ for Lin-42B, C, and AR242 5′-GTCTGTCCAACTGACCAGTAC-3′ and AR215 5′-GCCTGAAACGCC-TATCCGACGATG-3′ for Lin-42D. Lin-42D 5′RACE used AR238 5′-CTGTGCACATTCTCCAGACAG-3′.

Two additional transcripts detected by 5′RACE contained a 260-bp exon, or a truncated version thereof, transcribed 1.1 kb upstream of exon β and spliced to exons 6–8. However, their analysis suggests that they do not encode proteins with sequence similarity to LIN-42C, D; there are no appropriately positioned AUG codons. These isoforms have not been pursued.

Sequence analysis

Protein alignments were performed with ClustalW (www.ebi.ac.uk/clustalw) (Chenna et al., 2003). The putative nuclear localization site in *lin-42* was identified using PROSITE (http://us.expasy.org/prosite/) (Hulo et al., 2004).

Transformation rescue

C. elegans transformations were performed as described (Mello et al., 1991). Constructs tested for rescue were injected at 5 ng/μl with *sur-5::gfp* (pTG96, 75 ng/μl; Yochem et al., 1998) or *str-1::gfp* (100 ng/μl; Troemel et al., 1997) as a coinjection marker. Animals scored for rescue were raised from eggs hatched in the presence of food.

RNA interference

Exons 4–6 (pJT7) or 6–9 (pJT27) were PCR-amplified from *lin-42* cDNA and cloned into pPD129.36. Double-strand RNA synthesis and microinjections were conducted as described (Kamath et al., 2001). For *let-7* experiments, *mnDp1/+*; *unc-3 let-7* (Meneely and Herman, 1981) young adults were injected, and their *unc-3 let-7* progeny were scored. For *lin-29* experiments, young adult *sqt-1 unc-4 lin-29/mnC1* animals were injected, and their *sqt-1 unc-4 lin-29* homozygous progeny and heterozygous siblings were scored. Balanced heterozygous progeny exhibited precocious phenotypes at a frequency similar to wild-type controls.

Antibody preparation and immunohistochemistry

Exons 8 and 9 were PCR amplified and cloned into pGEX-3X (pHG67; Smith and Johnson, 1988). The resulting GST::LIN-42 fusion protein was purified from bacterial lysates on a GST column. Polyclonal antibodies were raised in rabbits against this antigen (Pocono Rabbit Farms and Laboratories) and purified essentially as described (Perrone et al., 1998).

Synchronized worm populations (Sulston and Hodgkin, 1988) were fixed as described (Ahnn and Fire, 1994). Slides were incubated with α-42C/D (1:10 dilution) and MH27 (1:500) for 2 h at 37°C. Secondary antibody incubations were with Alexafluor 488-conjugated goat-anti-mouse (1:400; Molecular Probes) and Cy3-conjugated goat-anti-rabbit (1:400; Jackson Labs) for 1 h at 37°C. Samples were mounted with 10 μl of VECTASHIELD (Vector Laboratories) plus 1 μg/ml DAPI. Microscopy was as described (Abrahante et al., 1998).

Results

Multiple LIN-42 isoforms with extended homology to Per proteins

Initial characterization of the *lin-42* locus revealed a splicing pattern in accordance with the predicted gene F47F6.2, identifying a single mRNA species containing 5 exons that reside within an 8.9-kb fragment capable of rescuing a *lin-42* mutation, *mg152* (Lin-42A; Fig. 1B, C; Jeon et al., 1999). The lesions in six *lin-42* alleles mapped to exons 2–5, and RT-PCR experiments revealed trans-splice leader (SL1) sequences just upstream of the presumptive translational start, identifying the 5′ end of the message. These experiments also confirmed the predicted splice pattern and revealed no alternative splicing upstream of exon 5. However, through 3′RACE experiments, we have now found that *lin-42* is alternatively spliced from within exon 5 to yield two additional mRNA species, Lin-42B and Lin-42C (Fig. 1B). These splice forms contain exons 1–4 of Lin-42A, followed by 275 bases of exon 5 (exon 5*) spliced to exons of predicted gene F47F6.1, which begins approximately 3 kb downstream and is not contained within the *lin-42* rescuing fragment. The splice pattern downstream of exon 5 differs for Lin-42B and Lin-42C, and they are predicted to produce 51- and 65-kDa proteins, respectively. For simplicity, we will refer to the sequence between the 5′-most *Pst*I site and the *Eag*I site as the "upstream" region of *lin-42* and the sequence between the *Eag*I and *Xho*I sites as the "downstream" region (Fig. 1B).

Comparison of the *lin-42* locus between *C. elegans* and *Caenorhabditis briggsae*, two nematode species that diverged an estimated 100 million years ago (Stein et al., 2003), revealed that *C. briggsae* Lin-42A contains a stop codon shortly after the conserved exon 5* 3′ splice site. Thus, only a truncated version of LIN-42A could be made in this species, suggesting that transcripts containing exon 5* (Lin-42B and Lin-42C) may be more central to *lin-42* function.

Database analysis indicated that only the PAS/PAC domain of LIN-42A has striking similarity to other proteins (Jeon et al., 1999) and identified the Period family of circadian rhythm proteins as most similar. Comparison of LIN-42C with PER proteins revealed two additional regions of similarity, denoted the SYQ and LT domains after conserved amino acids in their N-termini (Fig. 2).

The lin-42 downstream region is independently expressed

Because exons 6–9 of Lin-42C correspond to exons of the predicted gene F47F6.1, we asked if F47F6.1 is independently expressed or if transcripts from this region always contain the upstream *lin-42* exons. 5′RACE experiments using reverse primers in exon 6 detected an additional splice form, Lin-42D (Fig. 1B). Lin-42D initiates with exon β, which contains 65 nt of 5′ untranslated sequence plus codons for 12 amino acids, and has the composition β-6-7-8-9, indicating that F47F6.1 can be expressed independently. This 32.5-kDa isoform lacks the PAS domain but contains the SYQ and LT domains (Fig. 2).

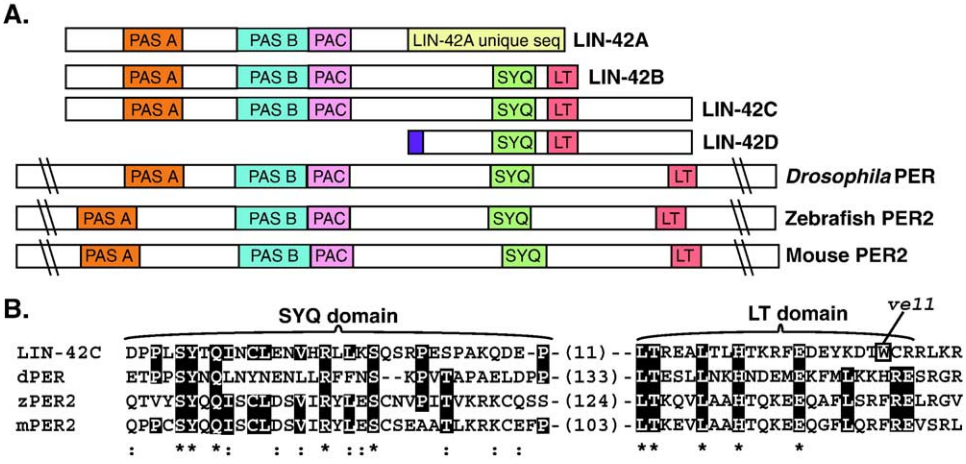

Fig. 2. LIN-42 shares multiple domains with PER proteins. (A) Stick diagrams of LIN-42A-D domain structure compared to fly (dPER), zebrafish (zPER2; Hirayama et al., 2003), and mouse (mPER2) PER proteins. The LIN-42A C-terminus (141 amino acids) and LIN-42D N-terminus (12 amino acids) are unique. (B) Alignment of the SYQ and LT domains. The first residue of the SYQ domain corresponds to amino acid 399 (LIN-42C), 609 (dPER), 653 (zPER2), and 579 (mPER2), respectively. Numbers in parentheses indicate the spacing between the domains. Dashes indicate spaces which optimize the alignments. Amino acids identical in three or more proteins are boxed. Residues conserved, or functionally similar, in all four proteins are marked with an asterisk and double dots, respectively. The residue mutated to a stop in *ve11* is indicated. LIN-42B terminates 4 amino acids prior to the end of the LT domain. The last 17 amino acids of the LIN-42C LT domain are a predicted bipartite nuclear localization signal (NLS). A similar motif beginning 30 amino acids downstream from the LT domain in flies has been shown to function as an NLS (Chang and Reppert, 2003). Genbank accession numbers are dPER, **P07663**; mPER2, **O54943**; zPER2, **NP_878277**.

ve11 contains a mutation in lin-42 coding sequence

Transgenic rescue of the *lin-42* mutant phenotype by a genomic fragment containing the upstream region (Jeon et al., 1999) raises the possibility that the downstream sequences are dispensable for function. However, the mutant lesion in one *lin-42* allele, *ve11*, was not found by sequencing exons 1–5. We discovered a single G-to-A transition that introduces a stop codon in exon 7 (Figs. 1B, 2) that would prematurely terminate translation of Lin-42B, C, and D transcripts, thereby implicating exons 6–9 in *lin-42* function.

ve11 was identified as a *lin-42* allele by its failure to complement *lin-42(n1089)* (Abrahante et al., 1998). *n1089* contains a large deletion that removes part of exon 2 and exons 3–5 (Fig. 1; see Materials and methods), therefore disrupting wild-type activity of *lin-42A*, *B*, and *C*, which could explain the failure of *ve11* and *n1089* to complement. However, the portion of intron 5 deleted in *n1089* may contain *lin-42D* promoter sequence, raising the possibility that this lesion affects the independent expression Lin-42D, and that the *ve11* phenotype is due solely to the loss of this downstream transcript. To test this idea, we asked whether the *mg152* allele, which creates a stop codon in exon 2, complements *ve11*. It does not. Thus, an allele capable of encoding only LIN-42D cannot provide *lin-42* function in trans to an allele capable of producing only LIN-42A. These results imply that Lin-42B or Lin-42C or both are important for wild-type *lin-42* function.

The downstream portion of the lin-42 locus is sufficient for rescue

Although the above analysis suggests that both the upstream and downstream regions are required for *lin-42* function, transgenes containing only upstream sequences (e.g., pMJ11 and pMJ13, Fig. 1C) can rescue the *lin-42(mg152)* lesion in exon 2 (Jeon et al., 1999). In light of the present analysis, these rescue results suggest that expression of LIN-42A from a multicopy array can replace the presumed loss of *lin-42A*, *B*, and *C* expression caused by the *mg152* mutation. We confirmed this result and showed that pMJ13 also rescues the *lin-42(n1089)* deletion (Fig. 1C; Table 1). In contrast, these clones failed to rescue *lin-42(ve11)*, indicating that presumed overexpression of upstream sequences are insufficient to rescue a downstream mutation.

In a reciprocal set of experiments, we assayed the rescuing ability of the downstream *lin-42* sequences. Surprisingly, pHG83, which contains the downstream genomic fragment, can rescue *mg152*, *n1089*, and *ve11* mutants (Fig. 1C; Table 1). Therefore, the downstream sequences can provide sufficient *lin-42* activity to rescue mutations in both the upstream and downstream regions and can compensate for loss of *lin-42A–D*. Further subclones reveal that sequence from exon 6 to 9 is key (pJT8, pJT9).

In summary, both the upstream and downstream regions of *lin-42* harbor rescuing activity in transformation experiments using multicopy arrays. Most intriguing is the rescue of *n1089* by pHG83 or pHG109. The *n1089* lesion deletes the LIN-42 hallmark, the PER-like PAS domain. Thus, this result indicates that the PAS domain is dispensable for LIN-42 function in the presence of multiple copies of the downstream region, emphasizing the importance of this region.

lin-42(RNAi) reveals more severe hypodermal phenotypes

Each of the seven *lin-42* alleles is predicted to produce at least one intact LIN-42 isoform, suggesting that they may be non-null. Indeed, *lin-42(n1089)* mutants occasionally have detectable levels of a LIN-42 antigen (see below). To determine whether more complete depletion of LIN-42 causes more penetrant or novel phenotypes, we performed RNA interference *(RNAi)* with dsRNAs that will target both upstream and downstream exons.

lin-42(RNAi) results in a hypodermal phenotype that is more penetrant than that of *lin-42* alleles: nearly 100% of the progeny of dsRNA-injected animals synthesize complete and robust adult cuticle during the L3 molt (Table 2). In contrast, the precocious alae phenotypes of *lin-42(n1089)*, *mg152*, and *ve11* mutants are incomplete; partial adult cuticle synthesis is observed in 28–48% of these L3 molt stage animals as revealed by gaps in their alae (Table 2). Although the *lin-42(RNAi)* hypodermal phenotype is more severe, no additional seam cell defects were observed. Seam cells executed wild-type division patterns until the L3 molt (n = 10–20 animals examined at each larval stage), and wild-type seam cell numbers were observed (Table 3).

lin-42 temporally patterns the vulva, gonad, and sex myoblasts

In addition to causing an enhanced hypodermal phenotype, *lin-42(RNAi)* also causes premature execution of developmental events not previously described for *lin-42* mutants. Specifically, the vulval precursor cells (VPCs), distal tip cells (DTCs), and sex myoblasts (SMs) precociously initiate late stage-specific events.

Wild-type VPCs divide in the mid-L3 stage to generate the 22 cells that comprise the vulva (Sulston and Horvitz, 1977). Although several other heterochronic mutants show precocious VPC divisions (Abrahante et al., 2003; Ambros and Horvitz, 1984), we have only observed this phenotype with one *lin-42* allele, *ve11*, and then only rarely (Table 2). However, *lin-42(RNAi)* resulted in precocious VPC divisions in 20–30% of animals (Table 2; Figs. 3A, B). Furthermore, only 17% of *ve11* and 0% of *mg152* and *n1089* adults had an everted vulva (Evl) phenotype, but *lin-42(RNAi)* caused this phenotype in over 40% of adults (Table 2).

lin-42(RNAi) also causes a precocious phenotype in gonad development. In wild-type hermaphrodites, the DTCs lead the migration of the gonad arms through a stereotypic developmental program (Fig. 3I) (Kimble and White, 1981). In the L2 and L3 stages, the DTCs are positioned ventrally, leading the anterior and posterior arms of the gonad as they elongate. In the late L3, the DTCs reorient and migrate dorsally over the lateral hypodermis. At the dorsal side, they reorient once more, turning back towards the mid-body, such that L3 molt gonads

Table 1
Rescue of the *lin-42* precocious alae phenotype

Construct[a]	Injected strain	Rescue quality[b]	Array	Percent transgenic animals with L3 molt alae[c]				Percent non-transgenic animals with L3 molt alae[c]			
				100%	25–95%	0–25%	*n*	100%	25–95%	0–25%	*n*
pTG96	*n1089*	–	*veEx320*	65	30	5	20	70	30	0	20
pMJ11	*ve11*	–	*veEx266*	89	5	5	19	100	0	0	7
		–	*veEx267*	59	29	12	17	80	20	0	30
pMJ13	*n1089*	+++	*veEx318*	4	36	59	22	35	55	10	20
		++	*veEx319*	14	59	32	22	45	55	0	22
		++	*veEx321*[d]	5	55	30	20	67	33	0	12
	ve11	–[e]									
pHG83	*n1089*	+	*veEx268*	20	70	10	20	74	26	0	19
		++	*veEx269*	0	65	35	20	65	30	0	20
		++	*veEx270*	20	55	25	20	85	15	0	20
	ve11[d,f]	+	*veEx322*	38	63	0	16	75	25	0	20
		+++	*veEx323*	4	17	78	23	100	0	0	10
		++	*veEx324*	15	50	35	20	90	10	0	20
pHG109	*n1089*	++	*veEx274*	20	60	20	20	70	30	0	20
		++	*veEx275*	20	60	20	20	67	33	0	15
		–	*veEx276*	76	16	8	25	83	17	0	18
	ve11[f]	+++	*veEx293*	5	45	50	22	75	25	0	12
		++	*veEx294*	17	54	29	24	82	18	0	11
pHG84	*mg152*	–	*veEx277*	70	20	10	20	50	50	0	4
		–	*veEx278*	82	12	6	17	66	34	0	29
	ve11	–	*veEx280*	61	22	17	18	83	17	0	18
		–	*veEx281*	83	11	6	18	94	6	0	18
pJT8	*n1089*	+	*veEx289*	40	50	10	20	81	19	0	21
		+	*veEx292*	40	45	15	20	88	6	6	17
	ve11[f]	++	*veEx299*	40	30	30	20	75	25	0	12
		++	*veEx300*	20	40	40	25	60	40	0	10
pJT9	*n1089*	–	*veEx284*	53	42	5	19	60	40	0	20
		–	*veEx291*	74	26	0	19	87	13	0	15
	ve11	–	*veEx302*	74	16	11	19	95	5	0	20
		–	*veEx303*	70	15	15	20	85	15	0	20

[a] Except where noted, *sur-5::gfp*, on pTG96, which programs GFP accumulation in nearly all somatic nuclei (Yochem et al., 1998), was used as a transformation marker.

[b] Strains were considered rescued if there was at least a 30% decrease in the percentage of transgenic animals with complete alae formation when compared to non-transgenic siblings. Rescue quality is determined by the percentage of animals within a rescued population that have L3 molt alae over 0-25% of seam cells: 0–20% (+), 20–50% (++), greater than 50% (+++). Animals that were highly mosaic as determined by *sur-5::gfp* expression were not scored.

[c] L3 molt animals were scored for the presence of adult alae on the cuticle and for GFP expression. Animals with continuous alae extending over all seam cells are classified as complete (100%). Animals with incomplete alae were subdivided based on percentage of alae present (25–95% or 0–25%). *n* = the number of animals for which one lateral side was scored.

[d] These arrays were generated with *str-1::gfp* (100 ng/μl), which is expressed in the AWB neurons (Troemel et al., 1997), as a marker.

[e] Three independent lines carrying an extrachromosomal array of pMJ13 failed to rescue the egg-laying defect of *ve11*, and presumably also the alae defect, but were not extensively scored because of the difficulty in maintaining non-rescuing arrays in the *ve11* background due to low brood size.

[f] The egg-laying defect of *ve11* was rescued in animals carrying the transgenic array.

have a characteristic just-reflexed appearance (Fig. 3E). During the L4 stage, the DTCs complete the migration back to the mid-body, forming an adult gonad with two U-shaped arms.

lin-42(RNAi) causes the DTCs to execute the reflex precociously, prior to the L2 molt, rather than during the late L3 (Table 2; Fig. 3D). They then continue to migrate towards the vulva, yielding an L3 molt stage gonad that resembles that of wild-type L4 molt animals (Fig. 3G). Although 0% of *n1089* mutants and less than 2% of *ve11* mutants exhibit precocious gonad turning at the L2 molt, at the L3 molt stage, the DTCs in these mutants have migrated significantly further towards the mid-body than do DTCs in wild-type animals of the same stage (Fig. 3F; Table 2).

Beginning in the mid-L3 larval stage, the two sex myoblasts (SMs) undergo three rounds of proliferative divisions that are easily monitored in animals bearing an *hlh-8::gfp* reporter gene (Harfe et al., 1998). In 18% of *ve11* animals, at least one SM precociously divided during the L2 stage (Table 2). Interestingly, only 3% of *lin-42(RNAi)* animals exhibited this phenotype, suggesting that the SMs may be somewhat resistant to *lin-42(RNAi)*. Reduced RNAi efficiency in this lineage has been previously observed (Fire et al., 1998).

LIN-42 levels oscillate with the molting cycles during postembryonic development

lin-42 transcript levels oscillate with the molting cycles, peaking during the intermolt (Jeon et al., 1999). To test for fluctuations in LIN-42 levels, we raised and purified polyclonal antibodies that should recognize the LIN-42C and D isoforms (α-42C/D). These antibodies reveal that LIN-42C/D is nuclear and broadly expressed (Figs. 4, 5). The specificity of the

Table 2
lin-42 phenotypic characterization

	L2 molt				L3 molt		Adult	
	Alae	Gonad[a]	VPC[b]	SM[c]	Alae[d]	Gonad Reflex[e] (*n*)	Egl[f]	Evl[g]
N2	0	0	0	0	0	27±7 (11)	0	0
mg152	0	0	0	n.d.	100 (48)	n.d.	44	0
n1089	0	0	0	n.d.	100 (35)	52±9 (14)	18	0
ve11	0	2[h]	8	18	100 (28)	50±11 (10)	96	17
lin-42(RNAi) (exons 4–6)	0	18	29	n.d.	100 (3)	n.d.	77	40
lin-42(RNAi) (exons 6–9)	0	32	20	2	100 (2)	124±22 (10)	100	43
gfp(RNAi)[i]	0	0	0	n.d.	0	25±8 (8)	0	0

All values are presented as a percent of total animals scored that had the indicated phenotype ($n \geq 20$ animals unless noted). n.d. (not determined).
[a] Percentage in which at least one gonad arm migrated to the dorsal side by the L2 molt.
[b] Percentage in which at least one VPC (vulval precursor cell) divided by the L2 molt.
[c] Percentage in which at least one SM (sex myoblast) divided by the L2 molt. Strains contained the integrated array *ayIs6*, which expresses *hlh-8::gfp* in the SMs (Harfe et al., 1998). $n=40$ for each genotype.
[d] Percentage with alae synthesis. For animals with alae, the percentage that had incomplete alae with gaps is indicated in parentheses. Alae were scored over seam cells H2-T.
[e] Distance from distal tip cell to outer edge of anterior gonad arm (μm).
[f] Animals were scored as egg laying defective (Egl) if their progeny hatched internally.
[g] Percentage with an abnormally everted vulva (Evl).
[h] The posterior gonad arm in one animal migrated dorsally, but then continued to grow posteriorly.
[i] dsRNA against the *gfp* gene was injected as a negative control.

antibody was demonstrated by the lack of signal in *lin-42(ve11)* mutant animals (Figs. 4N, O), which should terminate translation of Lin-42B, C, and D prior to the domain used to generate the antibody. Unexpectedly, *lin-42(mg152)* and *n1089* mutants, which presumably lack the LIN-A, B, and C isoforms, but are predicted to express LIN-42D, only occasionally stain with the antibody (e.g., for *n1089*, 3%; $n=100$). The essentially absent staining in *mg152* and *n1089* mutants suggests that either the upstream region is required for optimal accumulation of LIN-42D, or that endogenous LIN-42D levels are below the detection limit of the antibody. To ascertain the LIN-42D pattern independently of LIN-42C, we stained *lin-42(n1089)* animals which express *lin-42D* from an extrachromosomal array. LIN-42D was detectable in these animals, in a spatial and temporal pattern similar to that of wild type.

LIN-42 accumulates in nuclei with a dynamic temporal pattern during postembryonic development (e.g., compare Figs. 4A, D, F, M). Globally, LIN-42C/D accumulation is detected in essentially all somatic cell nuclei of intermolt animals and is undetectable in molting animals, even though both populations stain with a control antibody (MH27). Therefore, LIN-42C/D protein levels mirror message levels, peaking during the intermolt. However, within each larval stage, the LIN-42 pattern is complex; the timing of LIN-42 accumulation varies in different cell types, and the order in which cell types accumulate LIN-42 differs between stages as described below and summarized in Fig. 5Q.

L1 development

LIN-42 accumulation occurs in three distinct waves during L1 development. Between 7.5 and 12 h after N2 hatchlings are placed on food (Figs. 4A–E), LIN-42 accumulates in the nuclei of the hypodermis, pharynx (Figs. 4D, E), a few unidentified cells in the head and tail, and occasionally in the P neuroblasts (data not shown). Between 12 and 15 h, LIN-42 begins to accumulate in the intestine, body wall muscle, neurons, and the descendents of M (Figs. 4F, G). Next, between 15 and 18 h, LIN-42 accumulation begins in the somatic gonad (Figs. 4H, I). As L1 development nears the molt, LIN-42 staining disappears from the nuclei of most tissues, remaining only in 2–4 cells of the somatic gonad (Fig. 4J) and the nuclei of M.vlp (Fig. 4K) and M.vrp, cells that will eventually give rise to the SMs. Staining is undetectable in these lineages as the animals enter the molt.

L2 development

Similar to the L1 stage, the hypodermis (Fig. 5A), pharynx, and head and tail cells are among the first cells to accumulate LIN-42, and they do so shortly after the seam cells divide (22.5–24 h). The Pn.p cells, the anchor cell (AC), and ventral uterine cell (VU) (Fig. 5B) also show early LIN-42 accumulation. Between 24 and 26 h, a second wave is initiated, resulting in LIN-42 accumulation in most somatic cells, including the somatic gonad and distal tip cells (DTCs). Staining in all cell types persists until just prior to the L2 molt (29 h), when it coordinately disappears.

L3 development

After the L3 seam cell divisions (32–35 h), LIN-42 is again detected in the hypodermis, pharynx, head and tail cells, Pn.p cells, the somatic gonad, and the DTCs (Figs. 5C–F). The SMs begin to stain next (Figs. 5G, H), and then between 35 and 38 h, most other somatic cells accumulate LIN-42. LIN-42 persists in VPCs, SMs, and somatic gonad cells while they undergo mitosis (Fig. 5I). LIN-42 disappears from the somatic gonad after the first set of cell divisions and shortly thereafter from the DTCs, prior to the dorsalward turn, while remaining in all other somatic nuclei. The VPC daughters do not undergo their second division until after LIN-42 disappears. As the L3 molt nears, staining gradually disappears from all cells except the four SMs (Figs. 5J, K), where LIN-42 occasionally remains detectable after their second division (Figs. 5L), disappearing during the L3 molt.

Table 3
lin-42 RNAi in other heterochronic mutant backgrounds

Genotype	L2 molt		L3 molt			L4 molt
	Gonad[a]	VPC[b]	Gonad[c]	Seam cell #[d]	Alae[e]	Alae[e]
Wild type	0	0		15.8±0.4	0	100 (0)
lin-4				11.1±1.1	0	0
lin-42(ve11)				16.1±0.3	100 (28)	100 (0)
lin-4 lin-42(ve11)				12.1±1.2	0	100 (80)
Wild type (15°C)	0	0		15.8±0.5[f]	0	100 (0)
lin-42(RNAi) (15°C)	5	0		16.0±0.6[f]	100 (20)	100 (0)
lin-46 (15°C)	0	0		21.7±2.1[f,g]	0	100 (80)
lin-46; *lin-42(RNAi)* (15°C)	5	0		16.6±1.7[f,g]	100 (30)[h]	100 (10)[h]
lin-42(RNAi)	35	10			100 (0)	100 (0)
lin-46	5	0			0	100 (22)
lin-46; *lin-42(RNAi)*	25	10			100 (5)	100 (0)
lin-42(RNAi)	45	25	100 (3)	15.5±0.6	100 (0)	100 (0)
daf-12(rh62rh157)	0	0	95 (0)	25.9±1.7	0	100 (100)
daf-12(rh62rh157); *lin-42(RNAi)*	5	0	100 (10)	16.4±1.3	50 (100)	100 (40)
daf-12(rh61rh411)	0	0	83 (0)		0	100 (0)
daf-12(rh61rh411); *lin-42(RNAi)*	10	5	100 (10)		40 (100)	100 (40)
daf-12(rh61rh412)	0	0	95 (3)	19.3±1.5	0	100 (5)
daf-12(rh61rh412); *lin-42(RNAi)*	10	0	95 (26)	16.3±1.1	75 (100)	100 (40)
lin-42(RNAi)	55	10	100 (0)			
daf-12(rh61)			3 (0)			
daf-12(rh61); *lin-42(RNAi)*			2 (100)			
lin-42(RNAi)	15	15			100 (5)	100 (5)
unc-3	0	0			0	100 (0)
unc-3; *lin-42(RNAi)*	15	0			100 (0)	100 (5)
let-7 unc-3	0	0			0	50 (60)
let-7 unc-3; *lin-42(RNAi)*	10	0			35 (100)	95 (11)
lin-42(n1089); *let-7 unc-3*					20 (100)	95 (37)
lin-42(RNAi)	25	10			100 (5)	100 (0)
unc-4 sqt-1	0	0			0	100 (0)
unc-4 sqt-1; *lin-42(RNAi)*	25	15			100 (0)	100 (0)
unc-4 sqt-1 lin-29	0	0				0
unc-4 sqt-1 lin-29; *lin-42(RNAi)*	0	0			0	0

$n \geq 17$ animals scored for each phenotype.
[a] Percentage of animals executing dorsalward turn in at least one gonad arm by the L2 molt.
[b] Percentage of animals in which at least one VPC divided.
[c] Percentage of gonad arms executing the dorsalward turn. The number in parentheses indicates the percentage of gonad arms that turned dorsally but then migrated distally along the dorsal side.
[d] Number of seam cells±standard deviation. Each strain also contained *wIs78* to facilitate visualization of seam cells.
[e] Percentage of animals with adult alae. For animals with alae, the percentage that had incomplete alae with gaps is indicated in parentheses.
[f] Animals were homozygous for *unc-76*, which was used as a genetic marker to follow *lin-46* during strain construction.
[g] *lin-46(ma164)* was used for these assays; *lin-46(ma174)* was used for all other assays.
[h] Alae are less robust than in wild-type animals.

L4 development

LIN-42 reappears shortly after the L4 seam cell divisions (42–45 h) in the hypodermis, pharynx, a few head and tail cells, the vulva, and most cells of the somatic gonad, including the gonadal sheath cells (Figs. 5M, N). Notably, LIN-42 staining is never observed in the DTCs of L4 stage animals (Figs. 5O, P). Between 45 and 48 h, most other somatic cells stain while the hypodermal staining begins to disappear, correlating with onset of seam cell differentiation and fusion. As the animal enters the L4 molt, all staining disappears. Only rarely is LIN-42 detected in adults.

Genetic interactions in the hypodermis

Previous genetic analysis of *lin-42* used alleles that failed to eliminate completely LIN-42 activity. Using *lin-42(RNAi)*, we evaluated the relationship between *lin-42* and those components of the heterochronic pathway which cause retarded hypodermal phenotypes when mutated. Although we cannot rule out the possibility that *lin-42(RNAi)* leaves a low level of residual *lin-42* activity, the phenotypes observed following *lin-42(RNAi)* are more severe than those caused by *lin-42* alleles.

Seam cells of *lin-46* mutants fail to execute either the L2-L3 or the L4-adult transition (Pepper et al., 2004). At 15°C, seam cells in *lin-46* mutants reiterate the proliferative L2 division during the L3 larval stage (Fig. 1A) and subsequently fail to synthesize completely an adult cuticle at the L4 molt. In contrast, the seam cell lineage appears wild type at 20°C in *lin-46* mutants until the L4 molt when some seam cells fail to terminally differentiate. We found that *lin-46*; *lin-42(RNAi)* animals exhibited a precocious alae phenotype similar to that of *lin-42(RNAi)* at both 15°C and 20°C (Table 3). Furthermore, the

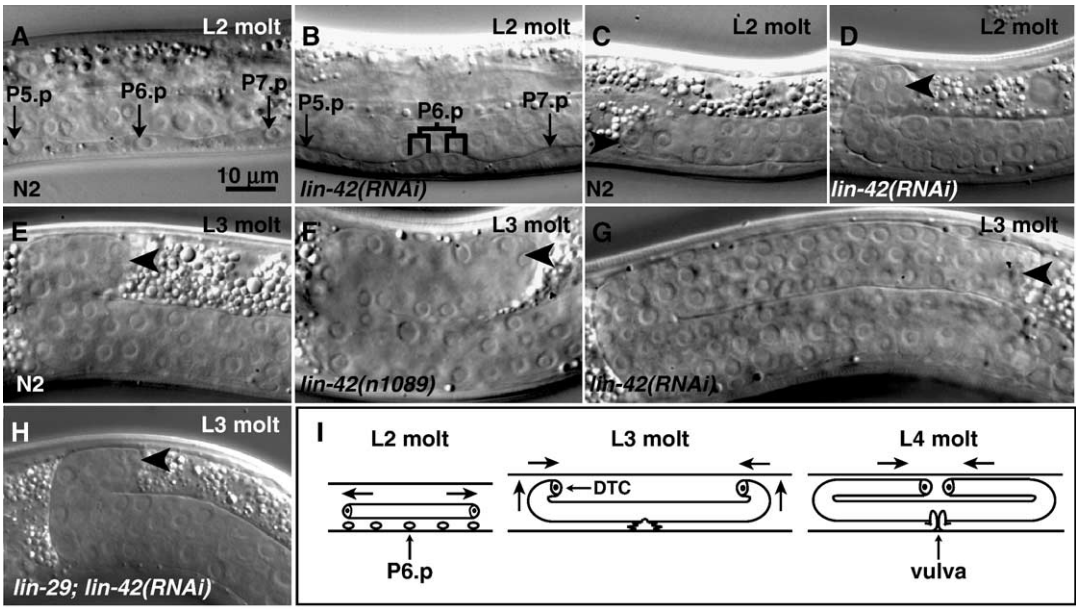

Fig. 3. Novel phenotypes revealed by *lin-42(RNAi*). In all micrographs, anterior is to the left and dorsal is at top. Vulval precursor cells (P5.p-P7.p) are undivided in wild-type L2 molt animals (A) but often divide by this stage in *lin-42(RNAi)* animals as in panel (B) where P6.p has divided twice. (C–H) Gonad morphology in wild-type and *lin-42(lf)* animals. Arrowheads indicate the distal tip of the anterior gonad arm. Gonad arms are positioned ventrally in wild-type L2 molt animals (C) but have often reflexed at this stage in *lin-42(RNAi)* animals (D) and appear similar to wild-type L3 molt gonads (E). *lin-42(n1089)* gonads extend significantly further back towards the mid-body relative to wild type (F) (see Table 2). L3 molt *lin-42(RNAi)* gonads (G) resemble that of wild-type L4 molt animals. (H) *lin-29*; *lin-42(RNAi)* gonads reflex at the L3 molt. dsRNA to exons 6–9 was used in these experiments. (I) Schematic of wild-type gonad morphogenesis.

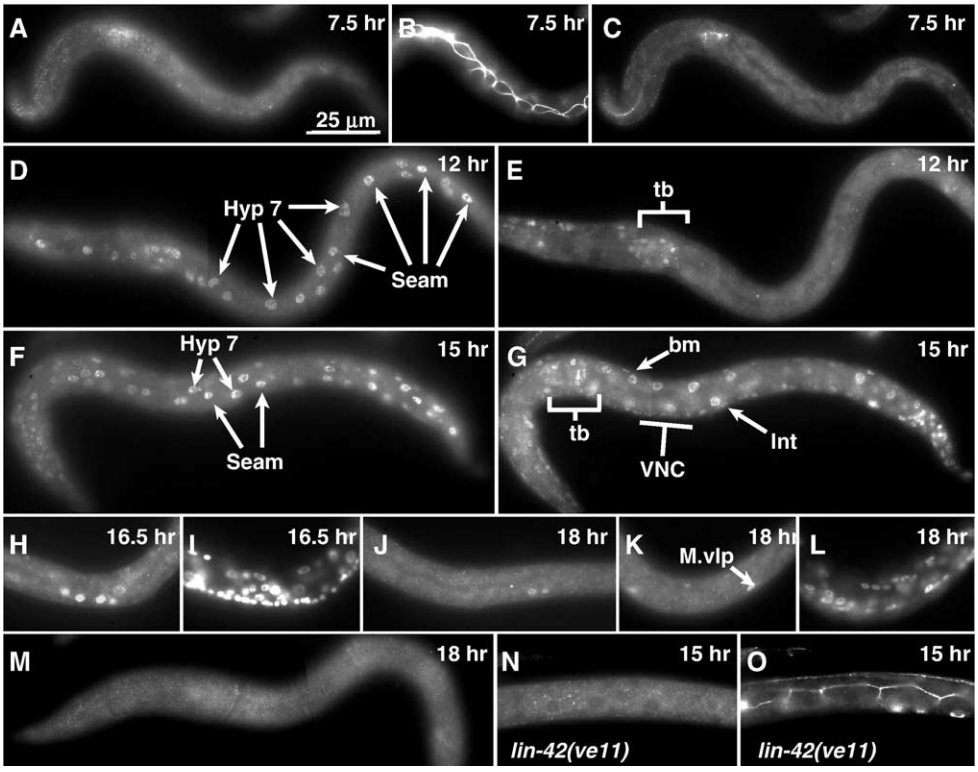

Fig. 4. LIN-42 accumulation in L1 stage animals. Time is indicated in hours after placement of synchronized L1s on bacteria. Here and in Fig. 5, animals are wild type, and LIN-42 is detected with α-42CD antibodies unless otherwise noted. LIN-42 is not observed at 7.5 h as demonstrated by focal planes through the hypodermis (A) and intestine (C). A control (B) shows the seam outlined by MH27 which detects the adherens junction-associated protein AJM-1 (Francis and Waterston, 1991). By 12 h LIN-42 is present in nuclei of seam cells and hyp7, the main body hypodermis (D), and additional cells in the head including the terminal bulb (tb) of the pharynx (E). At 15 h, LIN-42 is present in hypodermal and head cells (F), body wall muscles (bm), ventral nerve cord (VNC), intestine (Int), and unidentified tail cells (G). By 16.5 h LIN-42 levels have substantially decayed except in four somatic gonad nuclei (H). (I) DAPI staining of (H). LIN-42 persists in the somatic gonad (J), M.vlp (K) and M.vrp at 18 h, but is undetectable elsewhere (M). (L) DAPI staining of panel K. Background fluorescence levels, for example in panels A, C, and M, are not appreciably different from that of *lin-42(ve11)* mutants N. (O) Same animal as in panel N demonstrating permeability with MH27.

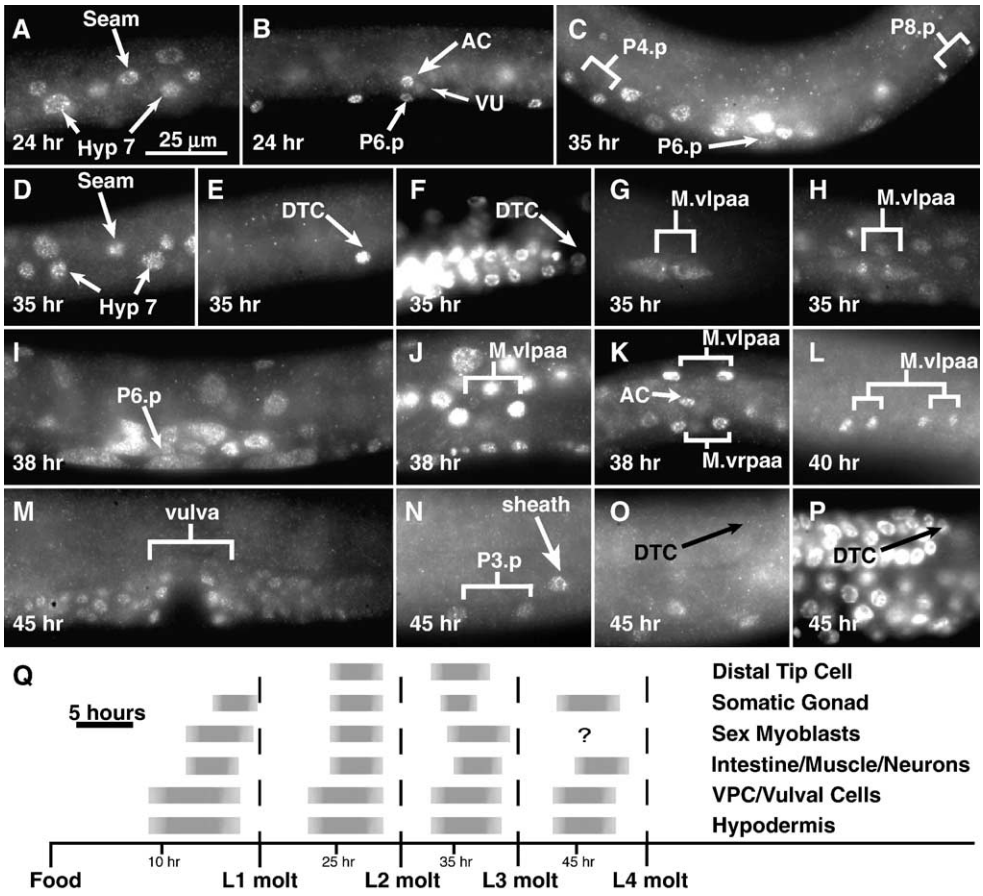

Fig. 5. LIN-42 accumulates in diverse cell types during late larval development. (A) LIN-42 throughout the hypodermis, in VPCs, the anchor cell (AC), and faintly in the ventral uterine cell (VU) in early L2s (B). Staining disappears during the molt and returns to these lineages in the L3 (C, D), when it also becomes detectable in the DTCs (E). (F) DAPI staining of panel E. *hlh-8::gfp* identifies an M descendent (G) which accumulates LIN-42 shortly after division (H). LIN-42 is present in Pn.p and somatic gonad cells during division (I). LIN-42 persists as the L3 molt nears (J) and is enriched in the SMs. (K) Ventral view of similar stage. In the late L3 (L), LIN-42 is only detected in the SMs. (M, N) LIN-42 in the vulva and somatic gonad of early L4s. DTCs do not accumulate LIN-42 after the L3 stage (O). (P) DAPI staining of panel O. (Q) Summary of postembryonic LIN-42 accumulation in a subset of cell types.

seam cell lineage of *lin-46*; *lin-42(RNAi)* animals was identical to *lin-42(RNAi)* animals, indicating that reiteration of the L2 division in *lin-46* mutants at 15°C requires LIN-42, and that *lin-42* acts downstream of *lin-46* with respect to both phenotypes. Although *lin-46*; *lin-42(RNAi)* animals raised at 15°C produce precocious alae at the same frequency as *lin-42(RNAi)* alone, the alae appear less robust, suggesting that *lin-46* may act through factors in addition to *lin-42* to control cuticle synthesis.

Similar to *lin-46* mutants, certain *daf-12* mutant animals also inappropriately reiterate the L2 division during the L3 stage, resulting in a retarded hypodermal phenotype (Antebi et al., 1998). We examined hypodermal development in three *daf-12* mutant backgrounds in which *lin-42* activity had been depleted by RNAi. *rh61rh411* and *rh61rh412* are predicted to eliminate the activities of all three DAF-12 isoforms, while *rh62rh157*, which exhibits a stronger L2 reiteration phenotype, could produce the B isoform with a mutation in the ligand binding domain (Antebi et al., 2000). *lin-42(RNAi)* restored a wild-type seam cell lineage to *rh61rh412* and *rh62rh157* mutant animals, indicating *lin-42* activity is also required for reiteration of the L2 proliferative division in *daf-12* mutants (Table 3). Loss of *daf-12* activity also significantly reduced the precocious hypodermal differentiation associated with *lin-42(RNAi)*; most seam cells in *daf-12*; *lin-42(RNAi)* animals differentiate after four molts, as in wild type, suggesting that these genes do not act in a linear pathway.

In contrast to *daf-12* and *lin-46* mutants, *lin-4* mutants have fewer seam cells than wild type due to omission of the L2 stage proliferative division as the L1 pattern reiterates (Chalfie et al., 1981). To examine the effects of *lin-42(lf)* on the *lin-4* phenotype, we used double mutants rather than RNAi due to the low brood size and egg-laying defects associated with *lin-4* alleles. As previously reported, *ve11*, the most severe *lin-42* allele, restores adult cuticle synthesis to the L4 molt in *lin-4* mutants (Table 3; Abrahante et al., 1998). We extended this analysis by examining seam cell lineage patterns and found that *lin-4 lin-42(ve11)* double mutants also fail to execute the proliferative L2 division. Thus, the ability of *lin-42* mutants to suppress the *lin-4* retarded hypodermal phenotype does not rely on restoration of a wild-type seam cell lineage (Table 3).

lin-42(n1089); *let-7(mn112)* mutants show mutual suppression, with a decreased penetrance of both the precocious *lin-42* phenotype and the retarded *let-7* phenotype (Reinhart et al., 2000). *let-7(mn112)*; *lin-42(RNAi)* animals exhibit a similar phenotype; although *lin-42(RNAi)* suppressed *let-7* more

completely than did *lin-42(n1089)*, it was nevertheless unable to form precocious alae in 65% of animals (Table 3).

Finally, *lin-29* is the most downstream component of the heterochronic pathway and is epistatic to *lin-42* alleles (Abrahante et al., 1998). Similarly, *lin-29*; *lin-42(RNAi)* animals failed to synthesize an adult cuticle at the L4 molt (Table 3).

Genetic interactions in the gonad

The precocious DTC migration phenotype observed in *lin-42(RNAi)* animals is unique among the described heterochronic mutants. However, certain classes of *daf-12* allele also affect gonad migration; the DTCs in these mutants sometimes fail to make the dorsalward turn at the L3 molt, and instead migrate into the head or tail (Antebi et al., 1998, 2000). This phenotype can be interpreted as developmental timing defect reiteration of the L2 stage migration pattern (linear ventral movement) which retards the turn. Because this phenotype is essentially opposite to that of *lin-42*, we performed *lin-42(RNAi)* in *daf-12* mutant backgrounds to examine their epistatic relationship. We used the three *daf-12* alleles described previously as well as *daf-12(rh61)* which has a highly penetrant gonad phenotype (Antebi et al., 2000).

lin-42(RNAi) produced a precocious gonad phenotype at the L2 molt in *daf-12(rh61rh411)*, *rh61rh412*, and *rh62rh157* mutant backgrounds, although with decreased frequency relative to *lin-42(RNAi)* alone (Table 3). In addition, the impenetrant failure of these *daf-12* mutants to execute the dorsalward turn was suppressed at the L3 molt. However, the gonads of many L3 molt *daf-12*; *lin-42(RNAi)* animals had a phenotype rarely seen in *lin-42(RNAi)* or *daf-12(lf)* alone; DTC migration was defective following the dorsalward turn. The DTCs in 10–25% of gonad arms reoriented incorrectly once they reached the dorsal side and instead migrated distally, perhaps reflecting an incomplete commitment to execution of the turn (Table 3). In contrast to strong *daf-12(lf)* alleles, *daf-12(rh61)*; *lin-42(RNAi)* gonads resembled those of *daf-12(rh61)* mutants, exhibiting a highly penetrant retarded phenotype, suggesting the *rh61* product hinders the turn.

We also examined the genetic relationship between *lin-29* and *lin-42* in gonad migration. LIN-29 appears in the DTCs just before the dorsalward turn (Bettinger et al., 1996), but *lin-29(lf)* mutations produce little or no gonad phenotype in hermaphrodites. *lin-42(RNAi)* did not cause a precocious dorsalward turn in a *lin-29(lf)* background (Table 3). Thus, wild-type *lin-29* activity is required for the precocious gonad phenotype in *lin-42* mutants.

Discussion

An expanded role for lin-42 in developmental timing

We demonstrate that the heterochronic gene *lin-42* times a broad array of events during postembryonic development. Not only does LIN-42 temporally pattern the hypodermis, but it also times events in the vulva, sex muscles, and somatic gonad. In these latter tissues, events that are normally restricted to the mid- (vulva, SMs) or late (gonad) L3 stage are executed one stage too early in animals lacking *lin-42* activity. Perhaps the most intriguing among these phenotypes is that of the somatic gonad, where *lin-42(RNAi)* causes the DTCs to lead the gonad arms in a precocious reflex at the L2, rather than L3 molt. This phenotype is a rare example of a temporal transformation in gonad morphology due to a disruption of the heterochronic pathway; temporal patterning of the DTCs appears unaffected in nearly all heterochronic mutants and has served as a guidepost by which to measure the passage of developmental time.

The other heterochronic gene known to time gonad migration is *daf-12*. Mutations in the *daf-12* nuclear hormone receptor fall into multiple phenotypic classes which correlate with lesions in particular protein domains, certain of which exhibit retarded heterochronic phenotypes in the gonad and seam (Antebi et al., 2000). Interestingly, these heterochronic phenotypes are impenetrant in *daf-12* null alleles but are highly penetrant for mutations in the ligand binding domain. This suggests that a DNA binding but ligand-insensitive mutant form of DAF-12 can interfere with the heterochronic gene pathway. The retarded gonad phenotype, in which the arms fail to reflex during the L3 molt, is nearly opposite to the *lin-42* precocious phenotype. Epistasis analysis showed that *lin-42(RNAi)* can induce precocious gonad turning, as well as precocious hypodermal and vulval defects, in the *daf-12* null background. However, these experiments revealed mutual suppression, rather than clear epistasis, suggesting that *daf-12* and *lin-42* may act in parallel branches of the heterochronic pathway.

Why is the *lin-42(RNAi)* gonad phenotype visible in the genetic background of *daf-12* null alleles but not *rh61*? One possibility is that *lin-42* and *daf-12* could act antagonistically through the same target genes, but that *rh61* acts dominantly to *lin-42*. The predicted ligand insensitive DAF-12 protein produced by *rh61* lacks a putative activation domain and can bind DIN-1, a corepressor (Ludewig et al., 2004). Thus, in one model, *rh61* has been postulated to have repressor activity but be unable to activate L3 stage programs (Antebi et al., 2000; Ludewig et al., 2004), which could cause the failure of the dorsalward turn even in the absence of *lin-42*.

Our experiments also revealed a role for *lin-29* in hermaphrodite gonad development, since LIN-29 is required for manifestation of the *lin-42(RNAi)* phenotype. This genetic relationship correlates with expression patterns; the disappearance of *lin-42* from the DTCs coincides with LIN-29 accumulation and initiation of dorsalward turn (Bettinger et al., 1996). Although their protein accumulation patterns are suggestive of autonomous roles within the DTCs, their foci of action could also be within body wall tissues over which the gonad migrates. The lack of fully penetrant gonad migration phenotypes in *lin-29* null and *lin-42(RNAi)* hermaphrodites suggests that a redundant mechanism acts to time the dorsalward turn. Interestingly, a variety of gonad migration defects are frequently observed in *lin-29* mutant males (Euling et al., 1999), indicating that this sex is more sensitive to *lin-29* activity.

A precocious gonad migration phenotype was previously observed in animals engineered to prematurely express UNC-5, a receptor for the UNC-6/netrin guidance cue (Su et al., 2000). Although premature UNC-5 accumulation in DTCs causes precocious execution of the dorsal turn, it appears qualitatively different from the *lin-42* phenotype; the DTCs continue to migrate centrifugally, such that they cross to the dorsal side at an oblique angle, and they continue to migrate beyond the normal reflex point before turning back towards the midline. Thus, early accumulation of UNC-5 appears to initiate precociously a single aspect of gonad migration, while *lin-42(RNAi)* causes a more complete temporal transformation, perhaps by activating multiple independent components of the migratory program.

In the hypodermis, epistasis experiments suggest that *lin-42* is more directly linked to *lin-46* activity than to *daf-12*. Although *lin-42(RNAi)* suppresses the reiterated proliferative division associated with both *lin-46* and *daf-12* alleles, it was epistatic only to *lin-46*. Thus, *lin-42* appears to act downstream in the *lin-46* branch (Pepper et al., 2004) of the heterochronic gene pathway to control the L2-to-L3 and L4-to-adult transitions, and it is likely to act in parallel to *daf-12* activity.

The dynamic and intricate expression patterns indicate a complex control mechanism for *lin-42*. Both message and protein levels oscillate, and it is thus likely that regulated half-lives of these molecules play a key role in modulation of *lin-42* activity. The elaborate LIN-42 accumulation pattern impedes simple assignment of its function. It is striking that *lin-42* is usually undetectable while most cells are actively dividing, and its accumulation pattern in several cell types makes it tempting to link *lin-42* with control of S-phase entry. For example, in the seam, *lin-42* disappears approximately when S-phase initiates and reappears shortly after cytokinesis. In the gut and main body hypodermis (hyp7), endoreduplication occurs near the molt (Hedgecock and White, 1985), when *lin-42* is also absent. However, *lin-42* mutants exhibit temporal transformations instead of obvious cell cycle defects. It is possible that potential cell cycle functions are undetected in *lin-42(lf)* backgrounds due to redundancy, similar to that of cell cycle regulators such as *lin-35* Rb, which does not produce a phenotype except in a sensitized background (e.g., Fay et al., 2002). Thus, although some correlation is apparent between the presence of *lin-42* and cell cycle phase, its significance remains unclear. Curiously, recent studies link cell cycle regulation to the circadian clock and PER function. For example, in developing zebrafish, a high percentage of cells enter S-phase at the end of the light period during a 24-h light–dark cycle, and when fish are raised under constant darkness, S-phase timing becomes asynchronous, suggesting circadian control (Dekens et al., 2003). Moreover, studies of mPer2 knockout mice reveal mis-regulation of cell cycle genes and suggest mPer2 acts as a tumor suppressor (Fu et al., 2002).

lin-42 is a complex locus

Our studies reveal that *lin-42* is a complex locus, encoding four distinct isoforms, and suggest that a bipartite structure underlies *lin-42* activity. Existing alleles affect two non-homologous regions of *lin-42* that are separable by transformation rescue experiments; genomic fragments containing either region can provide rescue activity. However, although constructs containing the downstream sequence alone can rescue mutations in either region, the reciprocal is not true; upstream constructs fail to rescue a downstream mutation.

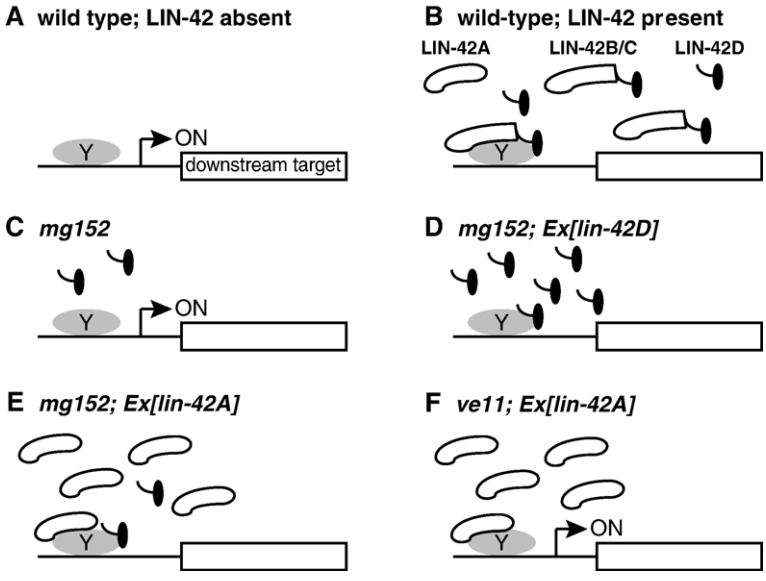

Fig. 6. Model for lin-42 action. (A–F) LIN-42 is predicted to function in a bipartite manner to interfere with transcriptional activator, Y. A domain in the LIN-42 C-terminus (present in LIN-42D) binds to Y and blocks its action (B, D, E), but this binding must be facilitated, which can be accomplished by LIN-42A (E) or by overexpression of LIN-42D (D). In the absence of facilitated binding of LIN-42D, Y is active (A, C, F). Rescue of *ve11*; *Ex[lin-42D]* would be repressive, similar to panel E, except with additional copies of LIN-42D. Y could be composed of multiple subunits and repressive interactions (B, D, E) may interfere with its DNA binding. Some LIN-42 isoforms could interact.

Based on the role of PER in other organisms (reviewed in Glossop and Hardin, 2002), we propose a model in which LIN-42 functions by interfering with transcriptional activator(s). In the absence of LIN-42, transcription factor Y leads to the expression of target genes (Fig. 6A). When LIN-42 is expressed, it interferes with the function of Y. The PAS domain in the N-terminus (LIN-42A, B, C) could help target the protein to Y, while the C-terminus (LIN-42B, C, D) might interfere more directly with its activity (Fig. 6B). This model must also incorporate our rescue data. That is, why does the downstream region rescue both upstream and downstream lesions whereas the upstream region cannot? One possible explanation is that the C-terminal domain is key to *lin-42* function, but that expression of endogenous LIN-42D alone does not provide the necessary level of downstream activity in the absence of LIN-42B and C (Fig. 6C), perhaps due to difficulty in targeting Y in the absence of the PAS domain. The concentration of LIN-42D may not be high enough to saturate binding sites, unless it is overexpressed from multicopy arrays (Fig. 6D).

If the downstream region is essential, why then can expression of the upstream region alone rescue *mg152* and *n1089*, which presumably cannot produce LIN-42A, B, C? A simple possibility is that overexpression of LIN-42A upregulates LIN-42D; however, antibody staining of transgenic animals does not support such a model. Instead, we favor the idea that overexpression of the PAS domain-containing LIN-42A lowers the threshold level required for downstream activity. LIN-42A binding to Y could increase its affinity for LIN-42D (Fig. 6E). The upstream region could still interact with Y in the presence of a downstream mutation, but in the absence of LIN-42D, the activity of Y is not effectively altered and transcription still occurs (Fig. 6F). Future work will be needed to distinguish between this and other models.

Because the downstream region is sufficient to rescue both classes of *lin-42* mutation when expressed from arrays, this region must serve a critical *lin-42* function. The newly identified *lin-42* exons in this region extend the homology between LIN-42 and PER proteins beyond the distinctive PAS domain. The SYQ and LT domains are also conserved in fly and vertebrate PER proteins, suggesting that they may be key to PER protein function in general; however, their functional importance has not been revealed through mutational analyses. The SYQ domain resides within a larger region required for fly PER interaction with cryptochrome (CRY), which mediates circadian photoreception (Rosato et al., 2001), but we do not detect a CRY homolog in worms. Intriguingly, the LT domain resides within a region that inhibits transcriptional activation by the CLOCK and CYCLE circadian rhythm proteins in cultured cells (Chang and Reppert, 2003). Further work is necessary to determine the function of the SYQ domain and to test whether the LT domain plays a direct role in the transcriptional regulatory activity of PER and perhaps LIN-42. Nevertheless, it appears that the PAS domain, the hallmark of Period-like proteins, may not be the most functionally significant feature of this protein family.

Acknowledgments

We thank Chris Gissendanner for helping with 5′RACE experiments, the CGC for worm strains, and Jeff Simon and Bob Herman for comments on the manuscript. Supported by NIH grants GM50227 to A.E.R. and HD007480 to J.M.T. and H.F.G.

References

Abrahante, J.E., Miller, E.A., Rougvie, A.E., 1998. Identification of heterochronic mutants in *Caenorhabditis elegans*: temporal misexpression of a collagen::green fluorescent protein fusion gene. Genetics 149, 1335–1351.

Abrahante, J.E., Daul, A.L., Li, M., Volk, M.L., Tennessen, J.M., Miller, E.A., Rougvie, A.E., 2003. The *Caenorhabditis elegans hunchback*-like gene *lin-57/hbl-1* controls developmental timing and is regulated by microRNAs. Dev. Cell. 4, 625–637.

Ahnn, J., Fire, A., 1994. A screen for genetic loci required for body-wall muscle development during embryogenesis in *Caenorhabditis elegans*. Genetics 137, 483–498.

Ambros, V., Horvitz, H.R., 1984. Heterochronic mutants of the nematode *Caenorhabditis elegans*. Science 226, 409–416.

Ambros, V., Horvitz, H.R., 1987. The *lin-14* locus of *Caenorhabditis elegans* controls the time of expression of specific postembryonic developmental events. Genes Dev. 1, 398–414.

Antebi, A., Culotti, J.G., Hedgecock, E.M., 1998. *daf-12* regulates developmental age and the dauer alternative in *Caenorhabditis elegans*. Development 125, 1191–1205.

Antebi, A., Yeh, W.H., Tait, D., Hedgecock, E.M., Riddle, D.L., 2000. *daf-12* encodes a nuclear receptor that regulates the dauer diapause and developmental age in *C. elegans*. Genes Dev. 14, 1512–1527.

Arasu, P.A., Wightman, B., Ruvkun, G., 1991. Temporal regulation of *lin-14* by the antagonistic action of two other heterochronic genes, *lin-4* and *lin-28*. Genes Dev. 5, 1825–1833.

Bettinger, J.C., Lee, K., Rougvie, A.E., 1996. Stage-specific accumulation of the terminal differentiation factor LIN-29 during *C. elegans* development. Development 122, 2517–2527.

Brenner, S., 1974. The genetics of *Caenorhabditis elegans*. Genetics 77, 71–94.

Chalfie, M., Horvitz, H.R., Sulston, J.E., 1981. Mutations that lead to reiterations in the cell lineages of *C. elegans*. Cell 24, 59–69.

Chang, D.C., Reppert, S.M., 2003. A novel C-terminal domain of *Drosophila* PERIOD inhibits dCLOCK:CYCLE-mediated transcription. Curr. Biol. 13, 758–762.

Chenna, R., Sugawara, H., Koike, T., Lopez, R., Gibson, T.J., Higgins, D.G., Thompson, J.D., 2003. Multiple sequence alignment with the Clustal series of programs. Nucleic Acids Res. 31, 3497–3500.

Cox, G.N., Laufer, J.S., Kusch, M., Edgar, R.S., 1980. Genetic and phenotypic characterization of roller mutants of *Caenorhabditis elegans*. Genetics 95, 317–339.

Dekens, M.P., Santoriello, C., Vallone, D., Grassi, G., Whitmore, D., Foulkes, N.S., 2003. Light regulates the cell cycle in zebrafish. Curr. Biol. 13, 2051–2057.

Euling, S., Bettinger, J.C., Rougvie, A.E., 1999. The LIN-29 transcription factor is required for proper morphogenesis of the *Caenorhabditis elegans* male tail. Dev. Biol. 206, 142–156.

Fay, D.S., Keenan, S., Han, M., 2002. *fzr-1* and *lin-35/Rb* function redundantly to control cell proliferation in *C. elegans* as revealed by a nonbiased synthetic screen. Genes Dev. 16, 503–517.

Feinbaum, R., Ambros, V., 1999. The timing of *lin-4* RNA accumulation controls the timing of postembryonic developmental events in *Caenorhabditis elegans*. Dev. Biol. 210, 87–95.

Fire, A., Xu, S., Montgomery, M.K., Kostas, S.A., Driver, S.E., Mello, C.C., 1998. Potent and specific genetic interference by double-stranded RNA in *Caenorhabditis elegans*. Nature 391, 806–811.

Francis, G.R., Waterston, R.H., 1991. Muscle cell attachment in *Caenorhabditis elegans*. J. Cell Biol. 114, 465–479.

Fu, L., Pelicano, H., Liu, J., Huang, P., Lee, C., 2002. The circadian gene Period2 plays an important role in tumor suppression and DNA damage response in vivo. Cell 111, 41–50.

Gissendanner, C.R., Crossgrove, K., Kraus, K.A., Maina, C.V., Sluder, A.E., 2004. Expression and function of conserved nuclear receptor genes in *Caenorhabditis elegans*. Dev. Biol. 266, 399–416.

Glossop, N.R., Hardin, P.E., 2002. Central and peripheral circadian oscillator mechanisms in flies and mammals. J. Cell Sci. 115, 3369–3377.

Hardin, P.E., Hall, J.C., Rosbash, M., 1990. Feedback of the *Drosophila* period gene product on circadian cycling of its messenger RNA levels. Nature 343, 536–540.

Harfe, B.D., Vaz Gomes, A., Kenyon, C., Liu, J., Krause, M., Fire, A., 1998. Analysis of a *Caenorhabditis elegans* Twist homolog identifies conserved and divergent aspects of mesodermal patterning. Genes Dev. 12, 2623–2635.

Hedgecock, E.M., White, J.G., 1985. Polyploid tissues in the nematode *Caenorhabditis elegans*. Dev. Biol. 107, 128–133.

Hirayama, J., Fukuda, I., Ishikawa, T., Kobayashi, Y., Todo, T., 2003. New role of zCRY and zPER2 as regulators of sub-cellular distributions of zCLOCK and zBMAL proteins. Nucleic Acids Res. 31, 935–943.

Hulo, N., Sigrist, C.J., Le Saux, V., Langendijk-Genevaux, P.S., Bordoli, L., Gattiker, A., De Castro, E., Bucher, P., Bairoch, A., 2004. Recent improvements to the PROSITE database. Nucleic Acids Res. 32, D134–D137.

Jeon, M., Gardner, H.F., Miller, E.A., Deshler, J., Rougvie, A.E., 1999. Similarity of the *C. elegans* developmental timing protein lin-42 to circadian rhythm proteins. Science 286, 1141–1146.

Kamath, R.S., Martinez-Campos, M., Zipperlen, P., Fraser, A.G., Ahringer, J., 2001. Effectiveness of specific RNA-mediated interference through ingested double-stranded RNA in *Caenorhabditis elegans*. Genome Biol. 2, 1–10.

Kimble, J.E., White, J.G., 1981. On the control of germ cell development in *Caenorhabditis elegans*. Dev. Biol. 81, 208–219.

Lee, R.C., Feinbaum, R.L., Ambros, V., 1993. The *C. elegans* heterochronic gene lin-4 encodes small RNAs with antisense complementarity to lin-14. Cell 75, 843–854.

Liu, Z., 1990. Genetic Control of Stage-specific Developmental Events in *C. elegans*. Harvard University.

Ludewig, A.H., Kober-Eisermann, C., Weitzel, C., Bethke, A., Neubert, K., Gerisch, B., Hutter, H., Antebi, A., 2004. A novel nuclear receptor/coregulator complex controls *C. elegans* lipid metabolism, larval development, and aging. Genes Dev. 18, 2120–2133.

Mello, C.C., Kramer, J.M., Stinchcomb, D., Ambros, V., 1991. Efficient gene transfer in *C. elegans*: extrachromosomal maintenance and integration of transforming sequences. EMBO J. 10, 3959–3970.

Meneely, P.M., Herman, R.K., 1981. Suppression and function of X-linked lethal and sterile mutations in *Caenorhabditis elegans*. Genetics 97, 65–84.

Moss, E.G., Lee, R.C., Ambros, V., 1997. The cold shock domain protein LIN-28 controls developmental timing in *C. elegans* and is regulated by the lin-4 RNA. Cell 88, 637–646.

Olsen, P.H., Ambros, V., 1999. The *lin-4* regulatory RNA controls developmental timing in *Caenorhabditis elegans* by blocking LIN-14 protein synthesis after the initiation of translation. Dev. Biol. 216, 671–680.

Pepper, A.S., McCane, J.E., Kemper, K., Yeung, D.A., Lee, R.C., Ambros, V., Moss, E.G., 2004. The *C. elegans* heterochronic gene *lin-46* affects developmental timing at two larval stages and encodes a relative of the scaffolding protein gephyrin. Development 131, 2049–2059.

Perrone, C.A., Yang, P., O'Toole, E., Sale, W.S., Porter, M.E., 1998. The *Chlamydomonas* IDA7 locus encodes a 140-kDa dynein intermediate chain required to assemble the I1 inner arm complex. Mol. Biol. Cell 9, 3351–3365.

Reinhart, B.J., Slack, F.J., Basson, M., Pasquinelli, A.E., Bettinger, J.C., Rougvie, A.E., Horvitz, H.R., Ruvkun, G., 2000. The 21-nucleotide *let-7* RNA regulates developmental timing in *Caenorhabditis elegans*. Nature 403, 901–906.

Rosato, E., Codd, V., Mazzotta, G., Piccin, A., Zordan, M., Costa, R., Kyriacou, C.P., 2001. Light-dependent interaction between Drosophila CRY and the clock protein PER mediated by the carboxy terminus of CRY. Curr. Biol. 11, 909–917.

Rougvie, A.E., 2005. Intrinsic and extrinsic regulators of developmental timing: from miRNAs to nutritional cues. Development 132, 3787–3798.

Rougvie, A.E., Ambros, V., 1995. The heterochronic gene *lin-29* encodes a zinc finger protein that controls a terminal differentiation event in *C. elegans*. Development 121, 2491–2500.

Ruvkun, G., Giusto, J., 1989. The *Caenorhabditis elegans* heterochronic gene *lin-14* encodes a nuclear protein that forms a temporal developmental switch. Nature 338, 313–319.

Seggerson, K., Tang, L., Moss, E.G., 2002. Two genetic circuits repress the *Caenorhabditis elegans* heterochronic gene *lin-28* after translation initiation. Dev. Biol. 243, 215–225.

Slack, F.J., Basson, M., Liu, Z., Ambros, V., Horvitz, H.R., Ruvkun, G., 2000. The *lin-41* RBCC gene acts in the *C. elegans* heterochronic pathway between the *let-7* regulatory RNA and the LIN-29 transcription factor. Mol. Cell 5, 659–669.

Smith, D.B., Johnson, K.S., 1988. Single-step purification of polypeptides expressed in *Escherichia coli* as fusions with glutathione S-transferase. Gene 67, 31–40.

Stein, L.D., Bao, Z., Blasiar, D., Blumenthal, T., Brent, M.R., Chen, N., Chinwalla, A., Clarke, L., Clee, C., Coghlan, A., Coulson, A., D'Eustachio, P., Fitch, D.H., Fulton, L.A., Fulton, R.E., Griffiths-Jones, S., Harris, T.W., Hillier, L.W., Kamath, R., Kuwabara, P.E., Mardis, E.R., Marra, M.A., Miner, T.L., Minx, P., Mullikin, J.C., Plumb, R.W., Rogers, J., Schein, J.E., Sohrmann, M., Spieth, J., Stajich, J.E., Wei, C., Willey, D., Wilson, R.K., Durbin, R., Waterston, R.H., 2003. The genome sequence of *Caenorhabditis briggsae*: a platform for comparative genomics. PLoS Biol. 1, E45.

Su, M., Merz, D.C., Killeen, M.T., Zhou, Y., Zheng, H., Kramer, J.M., Hedgecock, E.M., Culotti, J.G., 2000. Regulation of the UNC-5 netrin receptor initiates the first reorientation of migrating distal tip cells in *Caenorhabditis elegans*. Development 127, 585–594.

Sulston, J.E., Hodgkin, J., 1988. The Nematode *Caenorhabditis elegans* Methods. Cold Spring Harbor Laboratory Press.

Sulston, J.E., Horvitz, H.R., 1977. Post-embryonic cell lineages of the nematode, *Caenorhabditis elegans*. Dev. Biol. 56, 110–156.

Troemel, E.R., Kimmel, B.E., Bargmann, C.I., 1997. Reprogramming chemotaxis responses: sensory neurons define olfactory preferences in *C. elegans*. Cell 91, 161–169.

Wightman, B., Ha, I., Ruvkun, G., 1993. Posttranscriptional regulation of the heterochronic gene *lin-14* by *lin-4* mediates temporal pattern formation in *C. elegans*. Cell 75, 855–862.

Yochem, J., Gu, T., Han, M., 1998. A new marker for mosaic analysis in *Caenorhabditis elegans* indicates a fusion between hyp6 and hyp7, two major components of the hypodermis. Genetics 149, 1323–1334.